Published in final edited form as:
Mol Cell. 2007 October 26; 28(2): 200–213. doi:10.1016/j.molcel.2007.08.021.

Functional interdependence at the chromatin level between the MKK6/p38 and IGF1/Pi3K/AKT pathways during muscle differentiation

Serra Carlo[1,*], **Palacios Daniela**[2,*], **Mozzetta Chiara**[2], **Forcales Sonia V.**[1], **Morantte Ianessa**[1], **Ripani Meri**[1], **R. Jones David**[3], **Du Keyong**[4], **S. Jhala Ulupi**[5], **Simone Cristiano**[2,6], and **Puri Pier Lorenzo**[1,2,7]

1 *The Burnham Institute for Medical Research, 10901 North Torrey Pines Road La Jolla, CA 92037-1062*

2 *Dulbecco Telethon Institute (DTI) at Fondazione Santa Lucia/EBRI, Via di Fosso Fiorano, 64- 00143, Roma, Italy*

3 *Department of Surgery, University of Virginia, Charlottesville, VA 22908-0679*

4 *Molecular Oncology Research Institute, Tufts-New England Medical Center, 750 Washington St, Boston, MA 02111*

5 *The Whittier Institute, University of California-San Diego CA, CA 92037*

Abstract

During muscle regeneration, the mechanism integrating environmental cues at the chromatin of muscle progenitors is unknown. We show that inflammation-activated MKK6-p38 and IGF1-induced Pi3K/AKT pathways converge on the chromatin of muscle genes to target distinct components of the muscle transcriptosome. p38 α/β kinases recruit the SWI/SNF chromatin-remodeling complex; AKT 1 and 2 promote the association of MyoD with p300 and PCAF acetyltransferases, via direct phosphorylation of p300. Pharmacological or genetic interference with either pathway led to partial assembly of discrete chromatin-bound complexes, which reflected two reversible and distinct cellular phenotypes. Remarkably, Pi3K/AKT blockade was permissive for chromatin recruitment of MEF2-SWI/SNF complex, whose remodeling activity was compromised in the absence of MyoD and acetyltransferases. The functional interdependence between p38 and IGF1/Pi3K/AKT pathways was further established by the evidence that blockade of AKT chromatin targets was sufficient to prevent the activation of the myogenic program triggered by deliberate activation of p38 signaling

Introduction

Muscle regeneration occurs at the expense of myogenic progenitors (e.g. satellite cells), which are activated in response to myofiber injury (Wagers and Conboy 2005). The extensive genomic re-programming that occurs in the nuclei of satellite cells during the transition from quiescence to terminal differentiation is reflected in the dramatic changes of the chromatin at

7Corresponding author: Email: E-mail: lpuri@burnham.org and E-mail: plpuri@dti.telethon.it. Phone: 858-6463161 and +39 06-80319061.
*These authors equally contributed to the work
6Present address: Division of Medical Genetics, Department of Biomedicine in Childhood, University of Bari, Italy 70125

specific loci. For instance, the chromatin conformation at muscle-specific loci is repressive in undifferentiated, proliferating myoblasts, but becomes permissive for transcription at the onset of the differentiation program (Sartorelli and Caretti 2005; Palacios and Puri 2006). In contrast, the conformation of chromatin at the regulatory regions of proliferation genes is permissive for transcription in myoblasts, but precludes their expression in terminally differentiated myotubes (Ait-Si-Ali et al. 2004).

Satellite cell-mediated muscle regeneration is accompanied by the local release of several paracrine substances, e.g. cytokines, growth factors and hormones, as well as by cell-to-cell interactions, which are triggered upon muscle injury and the ensuing inflammatory response (Charge and Rudnicki 2004). These environmental cues govern satellite cell transition from quiescence to terminal differentiation by imparting to the chromatin of muscle loci the changes underlying this progression (Forcales and Puri 2006; Berkes and Tapscott 2005). Despite extensive knowledge of the intracellular cascades that transmit external cues to the nucleus, the molecular mechanism by which they are converted into chromatin modification at discrete loci remains largely unknown.

Recent studies have begun to analyze the composition of the transcriptosome that is assembled on the chromatin of muscle genes in response to the activation of the p38 kinases – the effectors of a pathway elicited in satellite cells by regeneration cues (Keren et al. 2006; Lluis et al. 2006). These studies have revealed that the p38 pathway promotes the assembly of a transcription-competent transcriptosome by recruiting the chromatin remodeling SWI/SNF complex to the regulatory regions of muscle genes (Simone et al. 2004a). Moreover, the p38 pathway regulates additional and related events, such a MyoD/E47 interactions (Lluis et al. 2005), MEF2 phosphorylation and activity (Zhao et al. 1999; Zetser et al. 1999; Ornatsky et al. 1999; Wu et al. 2000) and the RNA stability of selected myogenic transcripts (Briata et al. 2005).

Other signaling pathways elicited by regeneration cues cooperate with the p38 pathway in regulating the expression of genes implicated in the control of satellite cell differentiation. Among them, Pi3K/AKT signaling mediates satellite cell response to growth factors (e.g. IGF1) that promote critical events in the regeneration process, such as proliferation, muscle gene expression, myoblast fusion, survival and post-mitotic growth of myotubes (Musaro et al. 1999; Lawlor and Rotwein 2000; Rommel et al. 2001). Evidence of the functional impact of the IGF1-Pi3K-AKT pathway on muscle regeneration is also provided by *in vivo* studies (Musaro et al. 2001; Barton et al. 2002).

A number of downstream targets of the IGF1-Pi3K-AKT pathway have been identified (Sartorelli and Fulco 2004). However, the mechanism by which the IGF1-Pi3K-AKT pathway influences chromatin structure and chromatin-bound complexes of target genes in myoblasts is unknown.

Our previous studies showed that p38 and IGF1-Pi3K-AKT pathways proceed as two parallel promyogenic cascades in myoblasts induced to differentiate (Wu et al. 2000). Here we show that these two pathways converge at the chromatin level to control the assembly of the myogenic transcriptosome, by targeting two pharmacologically separable, yet functionally interdependent, events.

Results and Discussion

We used satellite cells derived from intact myofibers to investigate the impact of pharmacological blockade of p38 and IGF1/Pi3K on muscle regeneration. Upon culturing intact myofibers in mitogen rich medium (growth medium – GM), satellite cells delaminate and proliferate. Subsequent cell-to-cell contact together with mitogen withdrawal

(differentiation medium – DM) promotes their differentiation into multinucleated myotubes. Pharmacological blockade of the p38 kinases α and β, by SB203580 (SB), or the IGF-1/Pi3K/AKT pathway, by the Pi3K inhibitor LY294002 (LY), was achieved by the continuous exposure to the inhibitors throughout the transition from myofiber-associated satellite cells to myoblasts cultured in DM. Inhibition of either pathway prevented the expression of muscle-specific genes and precluded satellite cell fusion into myotubes with comparable efficiency (Fig. 1A and B). The same effects were also observed in established muscle cell lines, such as C2C12 cells (Suppl. Fig. 1A and B) and in primary cultures of human skeletal myoblasts (**data not shown**). However, the impact of SB and LY on the cell cycle machinery was different; only p38 blockade prevented the down-regulation of cyclin A that typically occurs during myotube formation (Fig. 1B). Furthermore, the undifferentiated myoblasts derived from the exposure to SB or LY during the incubation in DM showed striking morphological differences; SB-treated satellite cells appeared as elongated myoblasts, while LY-treated cells displayed rounded morphology (Fig. 1A) Both phenotypes could be readily distinguished from the typical morphology of normal, satellite cells. Comparable morphological effects were observed after simultaneous downregulation of individual p38 α and β or AKT 1 and 2 kinases, respectively, by RNA interference (RNAi) (Suppl. Fig. 1C, D, E and F). Thus, despite the shared ability to prevent the initiation of the differentiation program, pharmacological or genetic blockade of p38 and Pi3K resulted in biochemical and morphological differences, which likely reflect discrete chromatin signatures at specific loci. Consistent with this notion, we detected two unique patterns of histone acetylation at muscle loci in SB- vs LY-treated satellite cells (Fig. 1C) that reflect the assembly of two distinct chromatin-bound complexes with different enzymatic activity. Only Pi3K blockade prevented the local increase in histone acetylation on the regulatory elements of muscle genes **(**Fig. 1C), despite the global histone acetylation did not change in LY-treated satellite cells (Fig. 1D).

The results presented in Fig 1 suggest that the Pi3K/AKT and p38 pathways target different components of the muscle transcriptosome, and that the selective inhibition of either cascade can generate two populations of undifferentiated myoblasts showing distinct cellular phenotypes and discrete patterns of chromatin modification at muscle loci.

Based on this hypothesis, we carried out an extensive chromatin immunoprecipitation (ChIP) analysis to compare the assembly of the myogenic trancriptosome in myoblasts induced to differentiate in the presence of SB vs LY. We employed C2C12 myoblasts for this analysis, as they provided ample material necessary for ChIP. The chromatin of myoblasts in GM or DM, with and without SB or LY, was immunoprecipitated with antibodies against different components of the muscle transcriptosome and specific histone modifications. Consistent with Pi3K/AKT and p38 being parallel cascades delivering distinct external cues to discrete components of the myogenic transcriptosome, the composition of chromatin-bound complexes on myogenin promoter and muscle creatine kinase (MCK) enhancer was different in myoblasts exposed to SB or LY. SB selectively prevented the recruitment of the SWI/SNF complex, as previously reported (Simone et al 2004a). LY precluded the recruitment of p300 and PCAF acetyltransferases, and the consequent hyperacetylation on muscle promoters/enhancers (Fig. 2A). As hyperacetylation of MyoD increases its DNA binding affinity (Sartorelli et al. 1999), it was not surprising that in the absence of acetyltransferases, the majority of MyoD was hypoacetylated and hence unable to bind chromatin (Fig. 2A). By contrast, chromatin binding of MEF2A/C and SWI/SNF was not affected by LY treatment (Fig. 2A). The relative occupancy of Brg1, p300, PCAF, MyoD and the acetylation status of histone H3 were also quantified by real time PCR in independent experiments, which confirmed the differences reported above (Suppl. Fig. 2A and B). Interestingly, p38 α kinase was detected on the chromatin of target genes only in conditions permissive for differentiation (DM), regardless of the presence of SB or LY (Fig. 2A). In these conditions the large majority of p38 α is phosphorylated (Wu et al. 2000), suggesting the MKK3/6-dependent phosphorylation of p38

could be an important signal for chromatin recruitment. The presence of p38 on the chromatin of muscle genes in SB-treated cells is consistent with this scenario, as SB blocks the catalytic activity of p38α, without altering the phosphorylation status of this kinase. Notably, the effect of Pi3K blockade on the composition of chromatin-bound complexes appeared to be restricted to those muscle genes, whose expression was inhibited by LY. Indeed, p300 recruitment and histone hyperacetylation on the promoter of Atrogin-1, a catabolic gene repressed by IGF1 pathway (Stitt et al. 2004; Sandri et al. 2004), was not reduced, but rather increased in LY-treated myoblasts (Suppl. Fig. 2C and D).

The comparison of the effects produced by SB vs LY emphasizes the notion that these two cascades converge on the chromatin of muscle genes to target distinct components of the myogenic transcriptosome. The presence of the SWI/SNF complex in association with a transcriptional activator (MEF2) on the chromatin of muscle genes in LY-treated myoblasts raises the question of whether this complex is competent to remodel the chromatin at these loci. To address this issue we performed an endo-nuclease accessibility assay and found that, despite the different composition of chromatin-bound complexes in SB- and LY-treated myoblasts, both treatments precluded chromatin remodeling (Fig. 2B). This evidence demonstrates that the MEF2-SWI/SNF complex detected on the regulatory elements of muscle genes in LY-treated cells is not competent to remodel the chromatin.

Taken together these data reveal a functional interdependence between the p38 and Pi3K pathways at the chromatin level. The p38 pathway directs the recruitment of the SWI/SNF complex, but the ability of this complex to remodel the chromatin is conferred by the IGF-1/Pi3K pathway, via engagement of MyoD/acetyltransferases and consequent local hyperacetylation. In this regard, it is difficult to discriminate the role of MyoD as an essential factor for the recruitment of acetyltransferases (Yuan et al. 1996; Eckner et al. 1996; Puri et al. 1997a and b; Sartorelli et al. 1997) or as an independent regulator of SWI/SNF remodeling activity (Gerber et al. 1997; de la Serna et al. 2001).

Previous reports have documented the ability of MEF2 to form distinct complexes with transcriptional repressors (Miska et al. 1999; Lu et al. 2000). Consistently, immunoprecipitated MEF2A/C co-purified significantly higher deacetylase activity in LY-treated myoblasts, as compared to untreated or SB-treated myoblasts **(**Fig. 2C), and HDAC4 was found to be associated to MEF2A/C and SWI/SNF on the chromatin of muscle genes in LY-treated myoblasts **(**Fig. 2A). The reduced histone acetylation observed at the regulatory elements of muscle genes following Pi3K inhibition raised the possibility that these lysines were instead methylated. Recruitment of Polycomb-associated methyltransferase Ezh2 was previously reported to mediate silencing of muscle genes in undifferentiated myoblasts (Caretti et al. 2005). Indeed, the presence of the methyltransferase Ezh2 and its enzymatic effect - tri-methylation of H3 lysine K27 - was detected on the promoter of myogenin and the MCK enhancer in LY-treated myoblasts (Suppl. Fig. 3A). This finding suggests that the pharmacological blockade of Pi3K converts the conformation of the chromatin at muscle loci from permissive to repressive. The drastic changes in the components of the chromatin-bound complexes generated by LY treatment, which lead to histone lysine methylation, rather than acetylation and chromatin remodeling, also suggest that, in the absence of the IGF1 signaling, the MEF2-SWI/SNF complex associated with co-repressors could impose repressive chromatin modifications. We next tested whether the inhibition of the myogenic program by IGF1-Pi3K or p38 blockade is a stable or reversible epigenetic event. Suppl. figure 3B shows that the effects of SB and LY on muscle differentiation were readily reversible. These data indicate that is possible to generate a dynamic population of myoblasts with different chromatin conformation at muscle loci by pharmacological manipulation of signaling pathways.

The data presented in Fig. 2 suggest that the IGF1/Pi3K signaling affects the composition of the complexes bound to the chromatin of muscle genes both by promoting the recruitment of positive regulators (MyoD and acetyltransferases) and by preventing the engagement of co-repressors (histone deacetylases and methyltransferases). Given the importance of recruiting MyoD and acetyltransferases to enable the chromatin remodeling activity of SWI/SNF, we investigated the mechanism by which IGF1/Pi3K signaling promotes formation of the MyoD/acetyltransferase complex on the chromatin of muscle genes.

Interactions between MyoD and p300 are regulated at multiple levels (Puri and Sartorelli 2000). We first investigated the role of the IGF-1/Pi3K signaling in promoting physical interactions between MyoD and acetyltransferases in muscle cells, by co-immunoprecipitation studies with endogenous proteins. An association of MyoD with p300 and PCAF was detected in myoblasts induced to differentiate, and this complex was specifically disrupted by Pi3K inhibition (Fig. 3A). Simultaneous downregulation of indivudual kinases p38 α and β or AKT 1 and 2, respectively, by RNAi was also exploited to definitively assess the contribution of these kinases in regulating MyoD-p300 interaction. Although downregulation of either p38 α and β or AKT 1 and 2 (Fig. 3B) impaired the expression of muscle genes in differentiating myoblasts (Fig. 3C), only donwregulation of AKT1 and 2 prevented the association between endogenous MyoD and p300 (Fig. 3D). The interaction between MyoD and p300 was further measured by a mammalian two-hybrid system, by using a Gal4-luciferase reporter co-transfected with Gal4MyoD and p300 fused with the acidic activation domain VP16 (VP16p300). Exposure to IGF-1 in a serum-free medium stimulated the interaction between Gal4MyoD and VP16p300, and this effect was prevented by LY **(**Fig. 3E). By using two truncated versions of p300 (N-terminal aa1-744 and C-terminal aa871-2377), we established that the IGF-1 responsive region maps to the C-terminus (Fig. 3E). This finding is in agreement with the reported observation that the IGF1/Pi3K/AKT pathway promotes interaction between bHLH transcription factors and p300 during neurogenesis (Vojtek et al. 2003). Other works have reported on the ability of AKT to phosphorylate p300 (Huang and Cheng 2005). Indeed, two putative AKT consensus sites are present at the C-terminus of p300, within the MyoD interaction domain - the CH3 region. One consensus site (RRLS) maps to serine 1734 and is preferential for AKT1. The second phospho-acceptor site maps to serine 1834 (RRRMASM) and can be phosphorylated both by AKT1 and 2 **(**Fig. 3F). These sites are conserved in both p300 and CBP in different species. However, whether MyoD-p300 interaction is regulated via direct phosphorylation of p300 by AKT or by any other downstream kinase(s) has not been addressed by previous studies.

We monitored the phosphorylation pattern of endogenous p300 in myoblasts after metabolic labeling with ^{32}P orthophosphate and immunoprecipitation with anti-p300 antibodies. This analysis showed minimal fluctuations of global p300 phosphorylation along the transition from myoblasts to myotubes. However, Pi3K inhibition by LY significantly reduced the phosphorylation of p300 in myoblasts incubated in differentiation medium (DM) (Fig. 4A). This evidence further indicates the contribution of the IGF1/Pi3K pathway to p300 phosphorylation during myogenic differentiation. To precisely map the AKT phosphorylation sites in the p300 C-terminal, we expressed a HA-tagged truncated version of p300 (HA-1640-1840) in 293 cells along with constitutively active, myristoylated (myr) AKT1 or with inactive kinase death (kd) AKT1. After metabolic labeling with ^{32}P orthophosphate, the p300 HA-1640-1840 fragment was immunoprecipitated with anti-HA antibodies and subjected to phospho-peptide mapping (Fig. 4B). The two prominent spots detected in cells transfected with AKT1myr, but not in cells expressing AKT1 kd, were further subjected to phospho-aminoacid analysis, which revealed the presence of phospho-serines **(**Fig. 4C). The migration pattern of the phospho-peptides **(**Fig. 4B) and their confirmed identity by phospho-aminoacid analysis **(**Fig. 4C) are consistent with AKT-dependent phosphorylation of p300 on serines 1734 and 1834. Note that ectopic expression of AKT1myr correlated with the activation of

endogenous AKT2 (data not shown), suggesting a reciprocal activation and functional synergy between these two kinases. To confirm that these serines are phosphorylated *in vivo* during myoblast differentiation, we transfected the p300 C/H3 (p300 HA-1640-1840) fragment in C2C12 cells and monitored its phosphorylation after metabolic labeling with ^{32}P orthophosphate. An increased phosphorylation was observed in myoblasts induced to differentiate (Fig. 4D, compare lane 1 and 2, and Fig. 4E, compare lane 1 and 2). The ^{32}P incorporation was abrogated by either Pi3K inhibition with LY (Fig. 4D) or by replacement of the two serines with non-phosphorylatable alanines (p300 CH3 S1734/1834A) (Fig. 4E).

The phosphorylation of serine 1834 of endogenous p300 was further studied in human skeletal myoblasts (HSKM) using ser1834 phospho-specific antibodies (Liu et al. 2006). Immunofluorescence studies showed an increased nuclear staining in multinucleated, differentiated myotubes, as compared to undifferentiated myoblasts. Treatment with LY, but not SB, drastically reduced the nuclear accumulation of phosphoserine 1834 p300, although both compounds inhibited the formation of myotubes (Suppl. Fig. 4A). The changes in phosphorylation of serine 1834 of p300 in the conditions described above were confirmed by western blot on nuclear extracts (Suppl. Fig. 4B).

We next addressed the functional impact of AKT-mediated phosphorylation of p300 C-terminal serines 1734 and 1834 on p300-MyoD interaction, by using the mammalian two-hybrid-based assay shown in Fig. 3E. We compared the interaction of Gal4MyoD and the p300 C/H3 fragment, either wild type (VP16p300 C/H3 wt) or phospho-mutant (VP16p300 C/H3 S1734/1834A), fused to VP16. An interaction between Gal4MyoD and the VP16p300 C/H3 wt was observed in response to differentiation cues and was inhibited by LY. In the same conditions, the VP16-p300C/H3 S1734/1834A double mutant failed to interact with Gal4MyoD (Fig. 5A). Consistent with the role of AKT in promoting the association between MyoD and p300 via phosphorylation of the C/H3 domain of p300, co-transfection of the constitutively active form of AKT1myr, but not the AKT1 kd, was sufficient to promote interaction between Gal4MyoD and the VP16-p300 C/H3 wt, but not the VP16-p300C/H3 S1734/1834A mutant (Fig. 5B). The impact of each phosphoacceptor site on MyoD-p300 interaction was further analyzed by comparing the ability of full length Flag-tagged p300 wild type (wt) and single mutants (S1734A and S1834) to interact with endogenous MyoD, upon transient transfection in C2C12 myoblasts. Figure 5C shows that although these mutants are expressed at comparable levels (bottom panel), only p300 wt was found associated with MyoD (top panel). The relative impact of AKT1 and 2 on p300-MyoD interactions was also addressed by using mouse embryonic fibroblasts (MEFs) derived from AKT1 or AKT2 null mice (Liu et al. 2006). Employment of AKT 1 or 2 null cells eliminates the caveat intrinsic to the RNAi downregulation, consisting in the presence of residual, minimal expression level of the targeted isoform. We first monitored the binding of Gal4MyoD and VP16-p300 C/H3 wt in AKT1 and AKT2 deficient MEFs, as compared to wt MEFs. Absence of either AKT1 or AKT2 drastically impaired Gal4MyoD-VP16p300 interactions (Fig. 5D), further indicating that phosphorylation of p300 by both AKT1 and AKT2 is required for complex formation. In keeping with this conclusion, the interaction between endogenous p300 and ectopically expressed MyoD was detected in wt MEFs and in MEFs from MKK3/6 null mice, in which endogenous p38 cannot be activated (Brancho et al. 2003), but not in AKT1 null or AKT2 null MEFs (Suppl. fig. 5A). Consistently, the recruitment of MyoD and p300 to the chromatin of muscle genes was selectively impaired in MyoD-converted AKT1 or AKT2 null MEFs (Fig. 5E), while Brg1 was detected on the chromatin of these cells, but not in MyoD-converted MKK3/6 null MEFs **(**Fig. 5E).

Cooperation at the chromatin level between the Pi3K/AKT-mediated recruitment of MyoD and acetyltransferases and the p38-directed recruitment of SWI/SNF on the regulatory sequences of muscle genes was further explored by functional assays that combined deliberate

activation of p38 with inactivation of AKT chromatin effectors. The p38 pathway was activated in C2C12 myoblasts by the ectopic expression of the constitutively active form of its upstream kinase, MKK6EE-HA, via adenoviral delivery (Fig. 6A and B). These conditions resulted in the forced expression of muscle genes despite culture conditions non-permissive for differentiation (GM), and either p38 or Pi3K blockade was sufficient to prevent MKK6EE-induced muscle differentiation (Fig. 6A and B). While the effect of SB is expected, as this compounds blocks the downstream MKK6EE effector p38, the effect of LY was independent on the activation status of p38 (Fig. 6A and B). Consistent with the notion that the p38 and the IGF1/Pi3K/AKT pathways proceed as parallel cascades, which converge on different chromatin-bound complexes, the ability of LY to prevent MKK6EE-mediated activation of the myogenic program correlates with the local hypoacetylation and impaired chromatin remodeling at muscle loci (Fig. 6C and D). We next performed experiments aimed at establishing a direct relationship between MKK6EE-mediated activation of muscle gene expression and Pi3K/AKT-directed recruitment of p300 to the chromatin of muscle genes. In one experimental setting we compared the effect of the cytoplasmic inhibitor of the Pi3K/AKT pathway (LY) with that of the inhibitor of the Pi3K/AKT nuclear target p300 (the LysCoA) (Lau et al. 2000) on MKK6EE-dependent activation of the differentiation program in myoblasts. Figure 6E shows that microinjection of LysCoA at concentrations previously reported to inhibit p300 enzymatic activity (Lau et al. 2000; Polesskaya et al. 2002) was as efficient as LY in preventing the expression of myosin heavy chain (MyHC) in myoblasts injected with MKK6EE. These results establish a functional link between the p38 pathway and the integrity of the enzymatic activity of the Pi3K/AKT chromatin sensor p300. However, they do not address the specific role of AKT-mediated phosphorylation of p300 in the functional cooperation between the p38 pathway and p300. To this aim, we have compared the effect of over-expression of the truncated form of the C/H3 p300 (1640-1840), either wild type (wt) or the phospho-mutant (mt) ser1734/1834ala, on the ability of MKK6EE to promote the myogenic conversion in MyoD-expressing fibroblasts cultured in GM (Figure 6F). Increasing concentrations of C/H3 (1640-1840) wild type countered the ability of MKK6EE to promote myogenic conversion, but the effect was minimal with the phospho-mutant (Figure 6F). This result suggests that the dominant negative effect of C/H3 (1640-1840) fragment on muscle differentiation relies on the presence of AKT phosphorylation sites. Increasing concentrations of C/H3 (1640-1840) likely buffer the kinase availability of AKT toward endogenous p300. This evidence further supports the functional interdependence at the chromatin level between different enzymes, which are recruited into the myogenic transcriptosome by different signal-activated kinases, via direct phosphorylation.

Our results illustrate a model of cooperation between insulin/IGF1-activated signaling and the p38 pathway during skeletal myogenesis. In this model, IGF1-activated Pi3K/AKT signaling promotes the recruitment of MyoD and acetyltransferases to the chromatin of muscle genes, an event necessary to enable the chromatin remodeling activity of the p38-recruited SWI/SNF complex. Furthermore, our data suggest another, apparently distinct activity of IGF1 signaling, which is to displace or prevent the association of histone deacetylases and methyltransferases within the muscle transcriptosome. Selective interruption of IGF1/Pi3K/AKT signaling in conditions permissive for differentiation (DM), in which the p38 pathway is active, results in the formation of a complex containing MEF2 associated with co-repressors (i.e HDAC4, Ezh2), instead of co-activators (acetyltransferases) (**depicted in** Fig. 7). Indeed, MEF2-associated class II HDACs (Lu et al. 2000) and Ezh2-directed lysine methylation (Caretti et al. 2004) were reported to contribute to muscle gene silencing in myoblasts. Interestingly, the SWI/SNF complex can mediate repression of transcription, instead of activation, when associated to co-repressors (de la Serna et al. 2006;Marenda et al. 2004;Martens and Winston 2002). Further studies should establish whether p38-directed phosphorylation is involved in recruitment of SWI/SNF into repressive complexes. Likewise, it will be important to elucidate

the role of IGF1 signaling in the chromatin re-distribution of histone deacetylases and methyltransferases.

The terminal effectors of IGF1 signaling to the chromatin of muscle genes are AKT 1 and 2 kinases, which phosphorylate the C-terminal region of the acetyltransferase p300 at the onset of differentiation. The individual contribution of AKT 1 and 2 to the myogenic program is currently unclear, with works reporting on the essential role of AKT2, which is upregulated in differentiating myoblasts (Kaneko et al. 2002), and works reporting on the central role of AKT 1 in skeletal myogenesis (Wilson and Rotwein 2007). Our data indicate that AKT 1 and 2 are both necessary to phosphorylate p300 and promote interaction with MyoD and possibly other muscle specific transcription factors. Although the amino-acidic sequence of one p300 phospho-acceptor site (serine 1734) appears to be a preferential consensus for AKT 1 (Fig. 3F), our results indicate the requirement of both kinases for optimal phosphorylation of p300 C-terminal and the consequent interaction with MyoD. Genetic studies in MEFs deficient for either AKT 1 or 2 show that one kinase cannot compensate for the absence of the other (Fig. 5D, E and Suppl. Fig. 5A). Likewise, elimination of either phosphoacceptor site impairs the ability of p300 to interact with MyoD, as revealed by complementary assays (Fig. 5A, B and C). Conversely, expression of the constitutively active AKT 1 (AKT 1 myr) alone led to the phosphorylation of both serines 1734 and 1834, and this correlates with the activation of endogenous AKT 2 (data not shown). These results suggest that cross-activation between these two kinases might take place to achieve a cooperative effect on phosphorylation of common substrates (i.e. p300), although the biochemical basis for such synergy needs to be elucidated by future studies.

How does p300 C-terminal phosphorylation regulate the interaction with MyoD? Several mechanisms can cooperatively mediate this effect. The C/H3 domain is the region of p300 that mediates the interaction with MyoD (Yuan 1996, Eckner et al. 1996; Sartorelli et al. 1997). AKT-mediated C/H3 phosphorylation can induce/stabilize this interaction. MyoD and histone acetylation are additional events that promote MyoD/p300 binding and chromatin recruitment (Sartorelli et al. 1999; Polesskaya et al. 2001). As AKT-mediated phosphorylation was reported to stimulate the enzymatic function of p300 (Huang and Chen 2005), it is possible that an increased acetyltrasferase activity toward MyoD contributes to AKT-dependent interaction between MyoD and p300. Additionally, the C/H3 domain mediates interactions between p300 and pCAF (Yang et al. 1996), and AKT-mediated phosphorylation of p300 appears to contribute to the recruitment of pCAF, which in turn acetylates MyoD, p300 and histones to further stabilize the p300/MyoD/pCAF complex and activate transcription (Puri et al. 1997b; Sartorelli et al. 1999; Dilworth et al. 2004). Consistent with our results, others showed that inhibition of IGFII production in MyoD-converted fibroblasts precluded the engagement of p300 and PCAF on myogenin promoter (Wilson and Rotwein 2006). However, in their experimental setting chromatin recruitment of MyoD was not affected and the consequence on SWI/SNF enzymatic activity was not addressed.

The importance of AKT-mediated phosporylation of p300 extends to the regulation of SWI/SNF chromatin remodeling activity, as in the absence of MyoD/acetyltransferases the chromatin of muscle genes was hypoacetylated and un-remodeled, despite the presence of Brg1 (Fig. 2A and B). It is possible that histone acetylation is an event required for SWI/SNF to remodel chromatin, as nucleosomes containing acetylated histones are better predisposed for the enzymatic activity of of SWI/SNF (Chandy et al. 2006). The presence of SWI/SNF on hypoacetylated chromatin is apparently in conflict with previous works reporting on SWI/SNF chromatin binding via interactions of the bromodomain with acetylated histones (Hassan et al. 2001). However, according to a two-step model of SWI/SNF chromatin recruitment and activation, SWI/SNF can first be recruited by transcriptional activators, and then stabilized by interactions with acetylated histones. Local hyperacetylation (Chandy et al. 2006) and the

association with transcriptional activators (Gutierrez et al. 2007) appear to further promote the chromatin remodeling activity of SWI/SNF. Thus, in conditions in which acetyltransferases and MyoD are not recruited to the chromatin of muscle genes (i.e. interruption of Pi3K/AKT signaling), SWI/SNF recruitment by MEF2 (Fig. 2A and Suppl. Fig. 5B), in complex with deacetylases and methyltransferases (Fig. 2A, C and Suppl. Fig. 3A), could result in an impaired remodeling activity of SWI/SNF (Fig. 2B).

The interplay between two parallel signaling pathways at the chromatin levels may have a remarkable impact during the regeneration process. Both pathways are activated by regeneration cues and influence the ability of muscle progenitors to execute different stages of the regeneration program. The Pi3K/AKT pathway is elicited by locally released IGFs and promotes satellite cell proliferation, survival and differentiation (Mourkioti and Rosenthal 2005). The p38 pathway is activated in satellite cells, presumably in response to locally released inflammatory soluble factors or cell-to-cell interactions, and promotes cell cycle arrest (Puri et al. 2000; Perdiguero et al. 2007) and terminal differentiation (Zetser et al. 1999; Wu et al. 2000). The convergence of these two pathways at the chromatin level provides a mechanism for integration of regeneration cues to coordinate gene expression during cellular differentiation.

The different chromatin modifications observed in response to pharmacological inhibition of the p38 or the IGF1-activated pathways correlate with distinct cellular phenotypes in treated myoblasts. Pi3K blockade prevents the hyperacetylation of the chromatin of muscle genes, and leads to quiescence. p38 blockade promotes proliferation, which correlates with hypearcetylation at muscle genes (see illustration in Fig. 7). The acetylation status of the chromatin at muscle loci has a relevant biological impact during regeneration. For instance, MyoD acetylation regulates satellite cell capability to regenerate injuried muscles (Dunquet et al. 2006) and agents that increase histone hyperacetylation at muscle loci, such as deacetylase inhibitors, promote myogenesis *in vitro* and muscle regeneration *in vivo*, and revealed to be effective in the treatment of muscular dystrophies (Iezzi 2002;Iezzi 2004;Minetti 2006). Furthemore, deacetylase inhibitors can induce AKT activation in satellite cells (CM and PLP unpublished observation) and promote AKT-mediated phosphorylation of p300 in other cell types (Liu et al. 2006). Thus, the AKT signaling to chromatin-bound proteins, such as p300, could also contribute to the beneficial effects of deacetylase inhibitors on muscles regeneration.

Our results illustrate an example of convergence of distinct signaling pathways at the chromatin level, to coordinate the expression of genes implicated in satellite cell transition from quiescence to terminal differentiation. These data suggest potential pharmacological avenues for selective control of gene expression to manipulate muscle regeneration.

Methods

Cell cultures, plasmids, transfections, mammalian two-hybrid system and luciferase assay

C2C12 mouse myoblasts, 10T1/2 mouse fibroblasts converted by ectopic expression of MyoD were cultured in DMEM supplemented with 20% FBS (GM -growth medium) and switched to differentiation medium (DM - DMEM supplemented with 2% horse serum) or serum free medium (0.1 % FBS) supplemented or not with insulin growth factor 1 (IGF1) or insulin/transferrin when indicated. 293 cells were cultured in 10% FBS. Human skeletal myoblasts were purchased from Clonetics. Mouse embryonic fibroblasts (MEFs) were cultured in 10% FBS or switched to DM, when indicated.

Single muscle fibers with associated satellite cells were isolated as described (Minetti et al. 2006).

SB203580 and LY294002 were purchased from Calbiochem.

The p300 S1734A point mutant was made by quikchange using p300 WT pCI as a template. The Quikchange II XL kit from Stratagene was used with the following primers:

1734 Fwd - CGATTCTCGCCGCCTGGCTATCCAGCGCTGCATCCAG

1734 Rev – CTGGATGCAGCGCTGGATAGCCAGGCGGCGAGAATCG.

The p300 S1834A point mutant was described in (Liu et al. 2006)

Transfections were carried out with the Lipofectamine 2000 reagent and luciferase activity was determined with a Promega Luciferase kit and normalized by either β-Gal values or using the Dual–Luciferase reporter assay system (Promega). Mammalian two-hybrid system was performed as previously described (Sartorelli et al 1997), using p300VP16 constructs received from V. Sartorelli.

RNA interference

Simultaneous downregulation of AKT 1 and 2 or p38 α and β was achieved by RNAi using two distinct oligonucleotides specific to each isoform (Silencer Pre-designed siRNA from Ambion), as indicated in supplementare information. Oligonucleotide transfection of C2C12 was performed by using DharmaFETC 3 protocol and resulted in significant reduction (ranging from 80 to 90%) of targeted gene products.

Adenoviral Infections

Adenovirus expressing MKK6EE from the CMV promoter was described in (Simone et al. 2004a). C2C12 and MEFs were infected with pAdMKK6 for 2 hours in serum free medium and then placed in GM for additional 18 hours.

Gene expression analysis

Semi-quantitative RT-PCR was performed on RNA extracted from cells with Trizol (Invitrogen). The RNA was reverse transcribed and amplified by using the SuperScript One-Step RT-PCR (Invitrogen), according to standard procedures. For real time PCR, cDNA synthesis was performed from two independent RNA preparations using SuperScript III Platinum Two-Step qRT-PCR kit (Invitrogen) and High Capacity cDNA Archive Kit (Applied Biosystems) and quantitive PCR was performed with the ABI Prism 7500 PCR instruments (Applied Biosystems) to amplify samples in triplicate. PCR reactions were performed using the primers described in supplementary information.

Western blot was performed on cell extracts according to standard procedures. The following antibodies were used: anti-Ha (F7 from Santa Cruz), anti-total p38 and phospho-p38 (Cell Signaling), anti-myogenin (FD5 hybridoma), anti-acetylH3 (K9 and K14) (Upstate Biotechnology), anti-phospho 1834 p300 (Liu et al. 2006), anti total p300 (Santa Cruz n15) and anti-tubulin (Santa Cruz).

Microinjection studies and Immunofluorescence

Microinjection of C2C12 cells was performed as described in (Simone et al. 204a). Immunofluorescence studies on satellite muscle cells and human skeletal muscle cells were performed in paraformaldeide-fixed cells with the indicated antibodies.

Immunoprecipitation studies

Nuclear cell extracts and immunoprecipitations were performed as described in (Simone et al 2004). Briefly, nuclear extracts were pre-cleared with an A+G sepharose mix for 30 min at 4C and immunoprecipitated with agarose-conjugated anti-MyoD antibodies (M-318 Ac, Santa Cruz and RGB7 from Dr. S. Alemà). Precipitated proteins were revealed by western blot with anti-p300 (N15, Santa Cruz), anti-PCAF (H-369, Santa Cruz), and anti-MyoD (M-318, Santa Cruz) antibodies.

Metabolic labeling, phospho-peptide and phospho-aminoacid mapping

293T cells were transfected with HA tagged wt and mutant p300-CH3 (aa 1640-1840) constructs in the presence of kinase-dead of myristoylated Akt expression vectors. After 36 h, transfected cells were incubated with phosphate-free Dulbecco's modified Eagle medium containing 10% dialyzed serum and 1 mCi of [^{32}P]orthophosphate/ml. Following a 4hr incubation, the cells were washed with cold phosphate-buffered saline, and harvested in sodium dodecyl sulfate (SDS) lysis buffer (0.5% SDS, 50 mM Tris [pH 8.0], 1 mM EDTA) containing a cocktail of phosphatase inhibitors. The lysate was precleared with of pansorbin and supernatants were immunoprecipitated with agarose-conjugated anti-HA antibodies (Santa Cruz). Immunoprecipitates were resolved by SDS- gel electrophoresis, and transferred to nitrocellulose membranes. Following western blotting using HRP-conjugated (Santa Cruz) or AP-conjugated (Sigma) anti-HA antibodies, the HA-CH3 bands were excised, and subjected to tryptic digestion followed by 2-D phosphopeptide maps. Phosphopeptide maps were visualized by autoradiography. For phospho-aminoacid analysis, about 500 cpm of labeled peptides were oxidized in 6 N HCl, and heated to 110°C and the individual phosphoaminoacids were separated by two-dimensional high-voltage electrophoresis and visualized by ninhydrin staining and autoradiography.

Endonuclease Assay

Genomic DNA from C2C12 cells was extracted and used for endonuclease assay as previously described (Simone et al. 2004a). The primers used for PCR are described in supplementary information.

Deacetylase Assay

We used a Histone Deacetylase Assay Kit purchased from Upstate Biotechnology, as previously described (Simone et al. 2004a). C2C12 nuclear extracts were prepared as described and endogenous MEF2 A/D was immunoprecipitated by anti-MEF2 antibodies (Simone et al. 2004a). The MEF2-associated deacetylase activity was counted in a deacetylation assay by incubation with 60000cpm ^{3}H-acetylated H4 in 200ml 1x Assay buffer for 3h at 30C. 100nM trichostatin A (TSA) was used to inhibit deacetylase activity. Free ^{3}H-Acetyl was determined with liquid scintillation counting and results were adjusted to background.

Chromatin immunoprecipitation—A ChIP assay was performed as previously described (Simone et al. 2004a). The following antibodies were used: anti-MyoD (M-318 Ac, Santa Cruz), anti-MEF2c, anti-acetylated histone H4 (Upstate Biotechnology), anti-acetylated histone H3 (Upstate Biotechnology), anti-acetylated MyoD, anti-p300 (N-15 Ac, Santa Cruz), anti-PCAF (H-369, Santa Cruz), anti-p38 (received from Dr Sudo), anti-Brg1 (polyclonal N-15 and H-88, Santa Cruz), anti-HDAC4 (Santa Cruz). PCR was performed on immuno-precipitated DNA with the primers indicated in supplementary information.

Real-time PCR was performed using the SyberGreen Master Mix at least three times using three independent samples. Data reported in figures are values normalized to input DNA and

to values from normal rabbit IgG, which were set as the background (one unit) in each calculation. The primers used are indicated in supplementary information.

Supplementary Material

Refer to Web version on PubMed Central for supplementary material.

Acknowledgments

P.L.P is an associate Telethon scientist at Dulbecco Telethon Institute (DTI). We thank M. Birnbaum for providing AKT1 and 2 null MEFs, R. Davis for MKK3/6 double null MEFs, V. Sartorelli for p300VP16 constructs, P. Tsichlis for AKT constructs, P. Cole for LysCoA, and S. Alema for anti MyoD antibodies (RGB7). This work was supported by Telethon grant, RO1 NIH grant, Muscular Dystrophy Association grant (MDA), Parent Project and Compagnia San Paolo di Torino to PLP. CM is supported by Parent Project fellowship. UJ was supported by grants from JDRF and Hillblom foundation

References

Ait-Si-Ali S, Guasconi V, Fritsch L, Yahi H, Sekhri R, Naguibneva I, Robin P, Cabon F, Polesskaya A, Harel-Bellan A. A Suv39h-dependent mechanism for silencing S-phase genes in differentiating but not in cycling cells. EMBO J 2004;23:605–15. [PubMed: 14765126]

Barton ER, Morris L, Musaro A, Rosenthal N, Sweeney HL. Muscle-specific expression of insulin-like growth factor I counters muscle decline in mdx mice. J Cell Biol 2002;157:137–48. [PubMed: 11927606]

Berkes CA, Tapscott SJ. MyoD and the transcriptional control of myogenesis. Semin Cell Dev Biol 2005;16:585–95. [PubMed: 16099183]

Brancho D, Tanaka N, Jaeschke A, Ventura JJ, Kelkar N, Tanaka Y, Kyuuma M, Takeshita T, Flavell RA, Davis RJ. Mechanism of p38 MAP kinase activation in vivo. Genes Dev 2003;17:1969–1978. [PubMed: 12893778]

Briata P, Forcales SV, Ponassi G, Corte G, Chen C-Y, Karin M, Puri PL, Gherzi R. p38-dependent phosphorylation of the mRNA decay-promoting factor KSRP controls the stability of select myogenic transcripts. Mol Cell 2005;20(6):891–903. [PubMed: 16364914]

Caretti G, Di Padova M, Micales B, Lyons GE, Sartorelli V. The Polycomb Ezh2 methyltransferase regulates muscle gene expression and skeletal muscle differentiation. Genes Dev 2004;18:2627–38. [PubMed: 15520282]

Chandy M, Gutierrez JL, Prochasson P, Workman JL. SWI/SNF displaces SAGA-acetylated nucleosomes. Eukaryot Cell 2006;10:1738–47. [PubMed: 17030999]

Charge SB, Rudnicki MA. Cellular and molecular regulation of muscle regeneration. Physiol Rev 2004;84:209–38. [PubMed: 14715915]

de la Serna IL, Carlson KA, Imbalzano AN. Mammalian SWI/SNF complexes promote MyoD-mediated muscle differentiation. Nat Genet 2001;27:187–190. [PubMed: 11175787]

de la Serna IL, Ohkawa Y, Imbalzano AN. Chromatin remodelling in mammalian differentiation: lessons from ATP-dependent remodellers. Nat Rev Genet 2006;7:461–73. [PubMed: 16708073]

Dilworth FJ, Seaver KJ, Fishburn AL, Htet SL, Tapscott SJ. In vitro transcription system delineates the distinct roles of the coactivators pCAF and p300 during MyoD/E47-dependent transactivation. Proc Natl Acad Sci U S A 2004;10:11593–8. [PubMed: 15289617]

Duquet A, Polesskaya A, Cuvellier S, Ait-Si-Ali S, Hery P, Pritchard LL, Gerard M, Harel-Bellan A. Acetylation is important for MyoD function in adult mice. EMBO Rep 2006;7:1140–6. [PubMed: 17028574]

Eckner R, Yao TP, Oldread E, Livingston DM. Interaction and functional collaboration of p300/CBP and bHLH proteins in muscle and B-cell differentiation. Genes Dev 1996;10:2478–2490. [PubMed: 8843199]

Forcales SV, Puri PL. Signaling to the Chromatin During Skeletal Myogenesis: Novel Targets for Pharmacological Modulation of Gene Expression. Sem Cell Dev Biol 2005;16:596–611.

Gerber AN, Klesert TR, Bergstrom DA, Tapscott SJ. Two domains of MyoD mediate transcriptional activation of genes in repressive chromatin: a mechanism for lineage determination in myogenesis. Genes Dev 1997;11:436–450. [PubMed: 9042858]

Gutierrez JL, Chandy M, Carrozza MJ, Workman JL. Activation domains drive nucleosome eviction by SWI/SNF. EMBO J 2007;26:730–40. [PubMed: 17235287]

Hassan AH, Neely KE, Workman J. Histone acetyltransferases complexes stabilize SWI/SNF binding to promoter nucleosomes. Cell 2001;104:817–827. [PubMed: 11290320]

Huang WC, Chen CC. Akt phosphorylation of p300 at Ser-1834 is essential for its histone acetyltransferase and transcriptional activity. Mol Cell Biol 2005;25:6592–6602. [PubMed: 16024795]

Iezzi S, Cossu G, Nervi C, Sartorelli V, Puri PL. Stage-specific modulation of skeletal myogenesis by inhibitors of nuclear deacetylases. Proc Natl Acad Sci 2002;99:7757–7762. [PubMed: 12032356]

Iezzi S, Di Padova M, Serra C, Caretti G, Simone C, Maklan E, Zhao P, Hoffman E, Puri PL, Sartorelli V. Deacetylase Inhibitors Increase Muscle cell Size by Promoting Myoblast Recruitment and Fusion Through Induction of Follistatin. Dev Cell 2004;5:673–84. [PubMed: 15130492]

Kaneko S, Feldman RI, Yu L, Wu Z, Gritsko T, Shelley SA, Nicosia SV, Nobori T, Cheng JQ. Positive feedback regulation between Akt2 and MyoD during muscle differentiation. Cloning of Akt2 promoter. J Biol Chem 2002;277:23230–5. [PubMed: 11948187]

Keren A, Tamir Y, Bengal E. The p38 MAPK signaling pathway: a major regulator of skeletal muscle development. Mol Cell Endocrinol 2006;252:224–30. [PubMed: 16644098]

Lau OD, Kundu TK, Soccio RE, Ait-Si-Ali S, Khalil EM, Vassilev A, Wolffe AP, Nakatani Y, Roeder RG, Cole PA. HATs off: selective synthetic inhibitors of the histone acetyltransferases p300 and PCAF. Mol Cell 2000;5:589–595. [PubMed: 10882143]

Lawlor MA, Rotwein P. Insulin-like growth factor-mediated muscle cell survival: central roles for Akt and cyclin-dependent kinase inhibitor p21. Mol Cell Biol 2000;20:8983–95. [PubMed: 11073997]

Liu X, Shi Y, Birnbaum MJ, Ye K, De Jong R, Oltersdorf T, Giranda VL, Luo Y. Quantitative analysis of anti-apoptotic function of Akt in Akt1 and Akt2 double knock-out mouse embryonic fibroblast cells under normal and stressed conditions. J Biol Chem 2006;281:31380–31388. [PubMed: 16923802]

Liu Y, Denlinger CE, Rundall BK, Smith PW, Jones DR. Suberoylanilide hydroxamic acid induces Akt-mediated phosphorylation of p300, which promotes acetylation and transcriptional activation of RelA/p65. J Biol Chem 2006;281:31359–68. [PubMed: 16926151]

Lluis F, Ballestar E, Suelves M, Esteller M, Munoz-Canoves P. E47 phosphorylation by p38 MAPK promotes MyoD/E47 association and muscle-specific gene transcription. EMBO J 2005;24:974–84. [PubMed: 15719023]

Lluis F, Perdiguero E, Nebreda AR, Munoz-Canoves P. Regulation of skeletal muscle gene expression by p38 MAP kinases. Trends Cell Biol 2006;16:36–44. [PubMed: 16325404]

Lu J, McKinsey TA, Zhang CL, Olson EN. Regulation of skeletal myogenesis by association of the MEF2 transcription factor with class II histone deacetylases. Mol Cell 2000;6:233–44. [PubMed: 10983972]

Marenda DR, Zraly CB, Dingwall AK. The Drosophila Brahma (SWI/SNF) chromatin remodeling complex exhibits cell-type specific activation and repression functions. Dev Biol 2004;267:279–93. [PubMed: 15013794]

Martens JA, Winston F. Evidence that Swi/Snf directly represses transcription in S. cerevisiae. Genes Dev 2002;16:2231–6. [PubMed: 12208846]

Minetti GC, Colussi C, Adami R, Serra C, Mozzetta C, Parente V, Illi B, Fortuni S, Straino S, Gallinari P, Steinkhuler C, Capogrossi M, Sartorelli V, Bottinelli R, Gaetano C, Puri PL. Functional and morphological recovery of dystrophic muscles in mice treated with deacetylase inhibitors. Nature Medicine 2006;12:1147–50.

Miska EA, Karlsson C, Langley E, Nielsen SJ, Pines J, Kouzarides T. HDAC4 deacetylase associates with and represses the MEF2 transcription factor. EMBO J 1999;18:5099–107. [PubMed: 10487761]

Musaro A, McCullagh KJ, Naya FJ, Olson EN, Rosenthal N. IGF-1 induces skeletal myocyte hypertrophy through calcineurin in association with GATA-2 and NF-ATc1. Nature 1999;400:581–5. [PubMed: 10448862]

Musaro A, McCullagh K, Paul A, Houghton L, Dobrowolny G, Molinaro M, Barton ER, Sweeney HL, Rosenthal N. Localized Igf-1 transgene expression sustains hypertrophy and regeneration in senescent skeletal muscle. Nat Genet 2001;27:195–200. [PubMed: 11175789]

Ornatsky OI, Cox DM, Tangirala P, Andreucci JJ, Quinn ZA, Wrana JL, Prywes R, Yu YT, McDermott JC. Post-translational control of the MEF2A transcriptional regulatory protein. Nucleic Acids Res 1999;27:2646–54. [PubMed: 10373581]

Palacios D, Puri PL. The epigenetic network regulating muscle development and regeneration. J Cell Physiol 2006;207(1):1–11. [PubMed: 16155926]

Perdiguero E, Ruiz-Bonilla V, Gresh L, Hui L, Ballestar E, Sousa-Victor P, Baeza-Raja B, Jardi M, Bosch-Comas A, Esteller M, Caelles C, Serrano AL, Wagner EF, Munoz-Canoves P. Genetic analysis of p38 MAP kinases in myogenesis: fundamental role of p38alpha in abrogating myoblast proliferation. EMBO J 2007;39:750–8.

Polesskaya A, Naguibneva I, Duquet A, Bengal E, Robin P, Harel-Bellan A. Interaction between acetylated MyoD and the bromodomain of CBP and/or p300. Mol Cell Biol 2001;21:5312–20. [PubMed: 11463815]

Polesskaya A, Naguibneva I, Fritsch L, Duquet A, Ait-Si-Ali S, Robin P, Vervisch A, Pritchard LL, Cole P, Harel-Bellan A. CBP/p300 and muscle differentiation: no HAT, no muscle. EMBO J 2001;20:6816–6825. [PubMed: 11726517]

Puri PL, Avantaggiati ML, Balsano C, Sang N, Graessmann A, Giordano A, Levrero M. p300 is required for MyoD-dependent cell cycle arrest and muscle- specific gene transcription. EMBO J 1997a; 16:369–383. [PubMed: 9029156]

Puri PL, Sartorelli V, Yang XJ, Hamamori Y, Ogrizko Howard B, Kedes L, Wang JYJ, Graessmann A, Nakatani Y, Levrero M. Differential roles of p300 and PCAF acetyltransferases in muscle differentiation. Mol Cell 1997b;1:35–45. [PubMed: 9659901]

Puri PL, Wu Z, Wood L, Bhakta K, Zhang P, Han J, Feramisco JR, Karin M, Wang JYJ. Induction of terminal differentiation by constitutive activation of p38 MAP kinase in Human Rhabdomyosarcomas. Genes Dev 2000;14:574–584. [PubMed: 10716945]

Puri PL, Sartorelli V. Regulation of muscle regulatory factors by DNA-binding, interacting proteins, and post-transcriptional modifications. J Cell Physiol 2000;185:155–173. [PubMed: 11025438]

Rommel C, Bodine SC, Clarke BA, Rossman R, Nunez L, Stitt TN, Yancopoulos GD, Glass DJ. Mediation of IGF-1-induced skeletal myotube hypertrophy by PI(3)K/Akt/mTOR and PI(3)K/Akt/GSK3 pathways. Nat Cell Biol 2001;3:1009–1013. [PubMed: 11715022]

Sandri M, Sandri C, Gilbert A, Skurk C, Calabria E, Picard A, Walsh K, Schiaffino S, Lecker SH, Goldberg AL. Foxo transcription factors induce the atrophy-related ubiquitin ligase atrogin-1 and cause skeletal muscle atrophy. Cell 2004;117:399–412. [PubMed: 15109499]

Sartorelli V, Huang J, Hamamori Y, Kedes L. Molecular mechanisms of myogenic coactivation by p300: direct interaction with the activation domain of MyoD and with the MADS box of MEF2C. Mol Cell Biol 1997;17:1010–1026. [PubMed: 9001254]

Sartorelli V, Puri PL, Hamamori Y, Ogrizko V, Nakatani Y, Wang JYJ, Kedes L. Acetylation of MyoD directed by PCAF is necessary for the execution of the muscle program. Mol Cell 1999;4:725–734. [PubMed: 10619020]

Sartorelli V, Fulco M. Molecular and cellular determinants of skeletal muscle atrophy and hypertrophy. Sci STKE 2004;2004

Sartorelli V, Caretti G. Mechanisms underlying the transcriptional regulation of skeletal myogenesis. Curr Opin Genet Dev 2005;15:528–35. [PubMed: 16055324]

Simone C, Forcales SV, Hill D, Imbalzano AL, Latella L, Puri PL. Differentiation-activated p38 Pathway Targets SWI/SNF Chromatin Remodeling Complex to Muscle-Specific Loci. Nature Genetics 2004a; 7:738–43.

Simone C, Stiegler P, Bagella L, De Luca A, Sartorelli V, Giordano A, Puri PL. Deacetylase recruitment by the C/H3 domain of p300 acetyltransferase. Oncogene 2004b;12:2177–87.

Stitt TN, Drujan D, Clarke BA, Panaro F, Timofeyva Y, Kline WO, Gonzalez M, Yancopoulos GD, Glass DJ. The IGF-1/PI3K/Akt pathway prevents expression of muscle atrophy-induced ubiquitin ligases by inhibiting FOXO transcription factors. Mol Cell 2004;14:395–403. [PubMed: 15125842]

Tapscott SJ. The circuitry of a master switch: Myod and the regulation of skeletal muscle gene transcription. Development 2005;132:2685–95. [PubMed: 15930108]

Vojtek AB, Taylor J, DeRuiter SL, Yu JY, Figueroa C, Kwok RP, Turner DL. Akt regulates basic helix-loop-helix transcription factor-coactivator complex formation and activity during neuronal differentiation. Mol Cell Biol 2003;23:4417–4427. [PubMed: 12808085]

Wagers AJ, Conboy IM. Cellular and molecular signatures of muscle regeneration: current concepts and controversies in adult myogenesis. Cell 2005;122:659–667. [PubMed: 16143100]

Wilson EM, Rotwein P. Control of MyoD function during initiation of muscle differentiation by an autocrine signaling pathway activated by insulin-like growth factor-II. J Biol Chem 2006;281:29962–71. [PubMed: 16901893]

Wilson EM, Rotwein P. Selective Control of Skeletal Muscle Differentiation by Akt1. J Biol Chem 2007;282:5106–5110. [PubMed: 17218321]

Wu Z, Woodring PJ, Wen F, Feramisco JR, Karin M, Wang JYJ, Puri PL. p38 and extra-cellular signal-regulated kinases regulate the myogenic program at multiple steps. Mol Cell Biol 2000;20:3951–3964. [PubMed: 10805738]

Yang XJ, Ogryzko VV, Nishikawa J, Howard BH, Nakatani Y. A p300/CBP-associated factor that competes with the adenoviral oncoprotein E1A. Nature 1996;382:319–24. [PubMed: 8684459]

Yuan W, et al. Human p300 protein is a coactivator for the transcription factor MyoD. J Biol Chem 1996;271:9009–9013. [PubMed: 8621548]

Zetser A, Gredinger E, Bengal E. p38 mitogen-activated protein kinase pathway promotes skeletal muscle differentiation. Participation of the Mef2c transcription factor. J Biol Chem 1999;274:5193–200. [PubMed: 9988769]

Zhao M, New L, Kravchenko VV, Kato Y, Gram H, di Padova F, Olson EN, Ulevitch RJ, Han J. Regulation of the MEF2 family of transcription factors by p38. Mol Cell Biol 1999;19:21–30. [PubMed: 9858528]

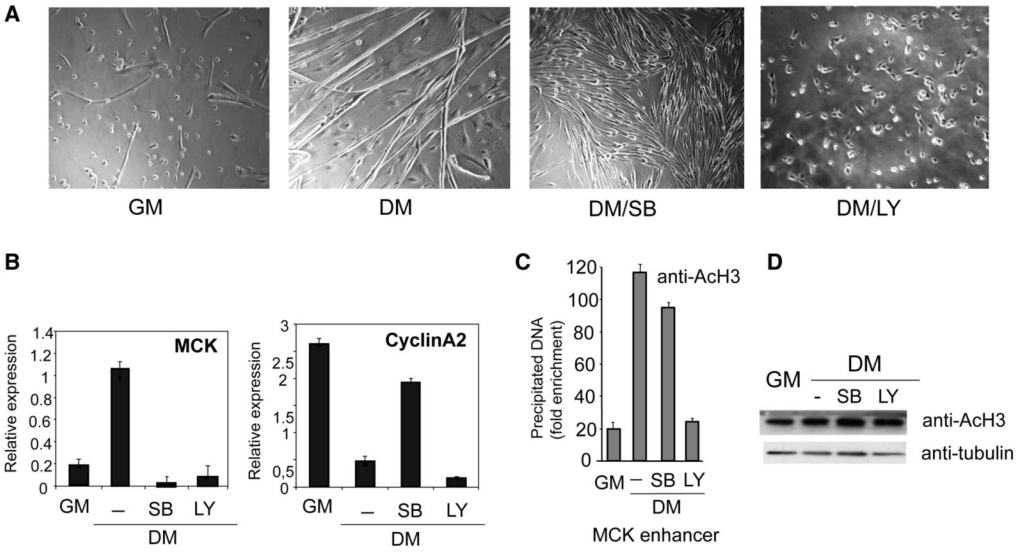

Fig. 1. Pharmacological blockade of p38 and Pi3K in satellite cells leads to distinct undifferentiated phenotypes

Myofiber were isolated from 3 month-old C57 mice and placed in culture (20% FBS, 10% horse serum, 1% chick embryo extract-contaning medium) in the presence or in the absence of SB (10μM) or LY (20 μM). The inhibitors were replaced by fresh compounds every 24 hours. During this time, in absence of the inhibitors, satellite cells delaminate and formed myotubes with high efficiency **A)** Effect of p38 and Pi3K blockade on satellite cell differentiation and morphology was evaluated by phase contrast microscopy **B)** Expression of MCK and Cyclin A2 transcripts was measured by real time PCR in satellite cells **C)** ChIP with anti-AcH3 antibodies was performed on chromatin of satellite cells. The reported data represent real-time RT-PCR values normalized to input DNA and to the values obtained with normal rabbit IgG **D)** Global H3 acetylation level was monitored by western blot from whole cell extracts of myofiber-derived satellite cells. The values shown in A and C represent the average of standard error of three independent experiments.

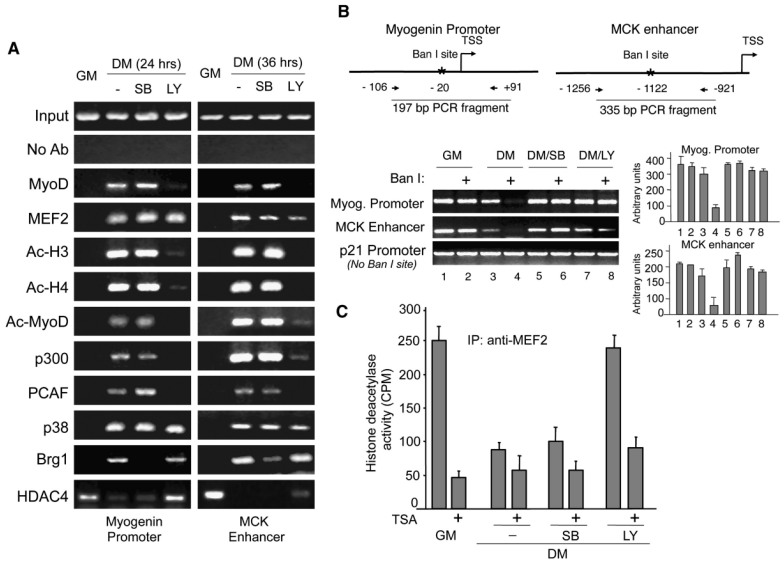

Fig. 2. Inhibition of Pi3K prevents the recruitment of acetyltransferases and MyoD on chromatin of muscle-regulatory genes

A) ChIP analysis of Ebox-containing regions within the myogenin promoter and MCK enhancer was performed on chromatin of C2C12 cultured in growth medium (GM – 20% FBS) or in differentiation medium (DM – Serum free/insulin transferring containing medium), using the indicated antibodies **B)** Endonuclease assay of myogenin promoter, MCK enhancer and p21 promoter in the same culture conditions as A. Restriction endonuclease accessibility was performed in nuclei by digestion with BanI, followed by PCR to amplify fragments relative to the transcription start site (TSS) of myogenin promoter (top panel, left) and MCK enhancer (top panel, right). As a control, a *p21* promoter fragment, which is devoid of *Ban I* sites was chosen. Absence or reduction of PCR signal indicates *Ban I* accessibility and reflects chromatin remodeling. The intensity of the amplified fragment was visualized (bottom panel, left) and quantified by densitometric analysis (bottom panel, right) **C)** MEF2-associated deacetylase activity was determined by deacetylation assay. Nuclear extracts from C2C12 cells undifferentiated (GM) or induced to differentiate (DM), with or without SB (5μM) and LY (20μM) were incubated with agarose-conjugated anti-MEF2A/D antibodies. Immunoprecipitates were incubated with tritium-labelled acetylated histones H4 and assayed for deacetylase activity, in presence or absence of the deacetylase inhibitor TSA (100nM). The values shown in B and C represent the average of standard error of three independent experiments.

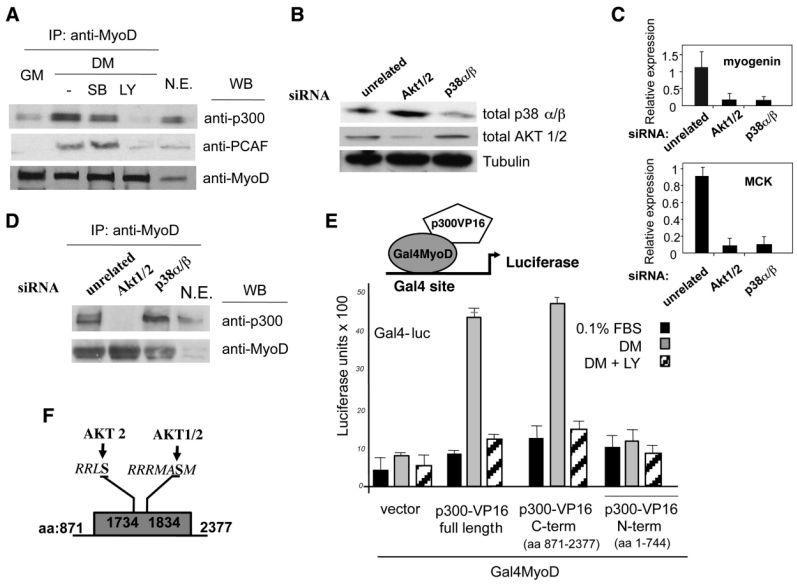

Fig. 3. Pi3K/AKT-dependent interactions between MyoD and the p300 C-terminus during myogenic differentiation

A) Immunoprecipitation of endogenous MyoD was performed from nuclear extracts of C2C12 myoblasts either undifferentiated (GM) or incubated in differentiation medium (DM) for 24 hours) in the absence or the presence of SB or LY. Levels of precipitated MyoD and co-precipitated p300 and PCAF were detected by western blot. Nuclear extracts (N.E.) from untreated DM cells was used as input **B)** Simultaneous downregulation of AKT 1 and 2 or p38 α and β was achieved in C2C12 cells by RNAi and was evaluated by western blot using antibodies detecting endogenous p38 α/β and total AKT. Specific reduction of expression (about 80%) of the targeted genes is shown, as compared to control cells (transfected with scrambled oligos) **C)** Expression of myogenin (top) and MCK transcripts (bottom) measured by real time PCR in C2C12 depleted of AKT 1 and 2 or p38 α and β, as shown in B **D)** Immunoprecipitation of endogenous MyoD was performed from nuclear extracts of C2C12 myoblasts depleted of AKT 1 and 2 or p38 α and β and incubated in differentiation medium (DM) for 24 hours. Levels of precipitated MyoD and co-precipitated p300 were detected by western blot **E)** The effect of Pi3K blockade on the interaction between p300 and MyoD in C2C12 myoblasts induced to differentiate in DM for 24 hours was evaluated by a mammalian two-hybrid assay. Activation of the reporter reflects interactions between Gal4MyoD and p300-VP16 **F)** Schematic representation of AKT phosphorylation sites in the c-terminal region of p300. The values shown in C and E represent the average of standard error of three independent experiments.

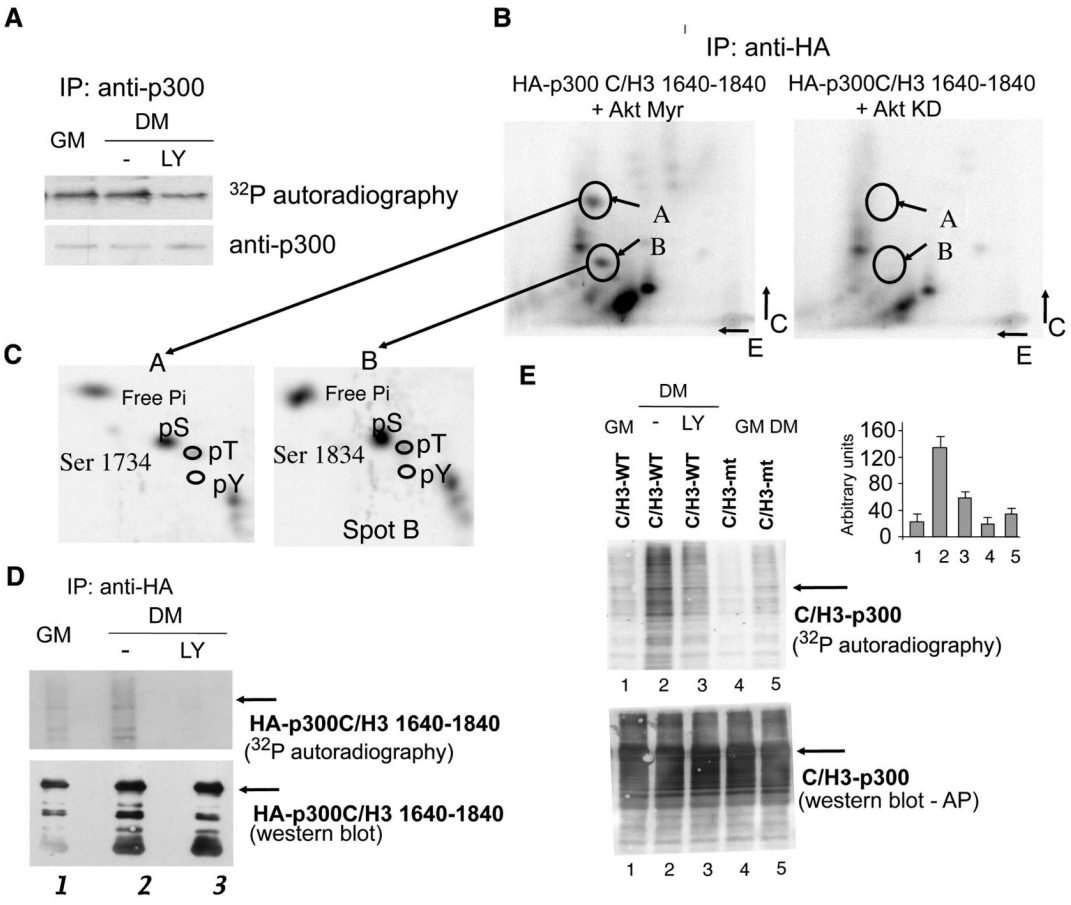

Fig. 4. Pi3K/AKT-dependent phosphorylation of the C/H3 domain of p300 during myogenic differentiation

A) Phosphorylation of endogenous p300 was evaluated after metabolic labelling with ^{32}P orthophosphate C2C12 myoblasts either undifferentiated (GM) or induced to differentiate (DM) in the absence or in the presence (lower panel) of LY. Endogenous p300 was immunoprecipitated with anti-300 antibodies. Top panel: ^{32}P incorporation is revealed by autoradiography; bottom panel: levels of immunoprecipitated p300 revealed by western blot **B)** Phosphopeptide mapping of HA-C/H3 1640-1840 of p300 with constitutively active AKT1 myristoylated (myr) or AKT1 kinase defective (k.d.). 293 cells were transfected with the HA-tagged p300C/H3 fragment (aa 1649-1840) along with either AKT myr or AKT k.d. After metabolic labelling with ^{32}P the C/H3-p300 was immunoprecipitated with anti-HA. Immunoprecipitates were subjected to SDS PAGE and then to phospho-peptide mapping **C)** Phospho-aminoacid analysis of the two most prominent spots detected in B after the bands were excissed **D)** Phosphorylation of HA-tagged C/H3-p300 in C2C12 myoblasts either undifferentiated (GM) or induced to differentiate (DM) in the absence or presence of LY. C2C12 myoblasts were transfetced with HA-tagged p300C/H3; after metabolic labelling with ^{32}P orthophosphate the C/H3 p300 was immunoprecipitated with anti-HA. Top: p32 incorporation is revealed by autoradiography; bottom: levels of immunoprecipitated p300 C/H3 revealed by anti-HA **E)** Phosphorylation of HA-tagged C/H3-p300 wild type (wt) in C2C12 myoblasts either undifferentiated (GM) or induced to differentiate (DM) in the absence or presence of LY, and the HA-C/H3-p300 phospho-mutant (mt). After transfection and metabolic labeling with ^{32}P orthophosphate the C/H3 p300 was immunoprecipitated with anti-HA. Top: ^{32}P incorporation is revealed by autoradiography; bottom: levels of immunoprecipitated

p300 CH3 revealed by anti-HA with alkaline phosphatase (AP) western blot. Quantification of two independent experiments was determined by densitometric analysis of the signal relative to the immunoprecipitated C/H3-p300 (see band indicated by arrow) and calculated as ^{32}P/AP signal ratio (right panel). The values represent the average of standard error of three independent experiments.

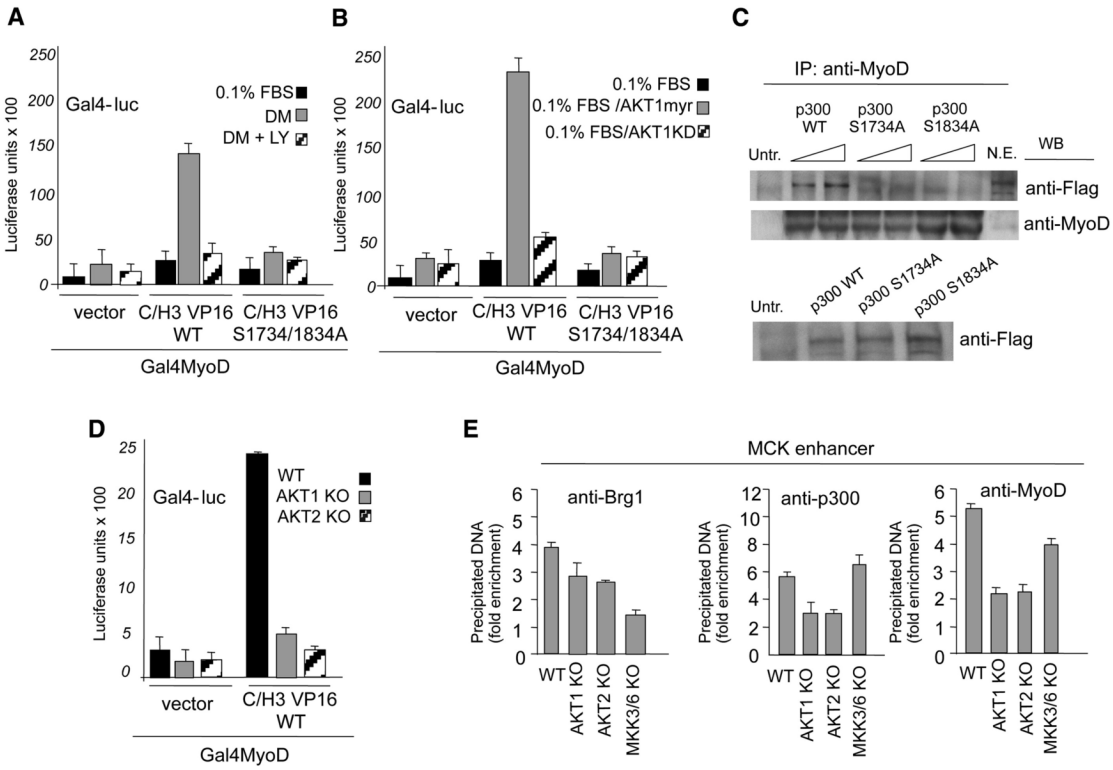

Fig. 5. Replacement of two potential AKT-target serines with non-phosphorylatable alanines or genetic ablation of one AKT isoform impairs the interaction between the p300 and MyoD during myogenic differentiation

The effect of differentiation cues **(A)** or the ectopic expression of constitutive active myristoylated AKT1 (myr) **(B)** on the interaction between Gal4-MyoD and the C/H3 domain of p300, either wt or the phospho-mutant (S1734/1834A) fused to VP16 (C/H3 VP16) was evaluated in C2C12 cells by a mammalian two hybrid assay, upon co-transfection with Gal4-luciferase reporter **C)** Co-immunoprecipitation of endogenous MyoD and ectopically expressed full length p300 wt and single mutants S1734A and S1834A performed in C2C12 cells after transfection of increasing concentrations (3 and 6 μg) of p300 mutants. Levels of precipitated MyoD and co-precipitated Flag-tagged p300 (top panel) were detected by western blot. Bottom panel shows total level of Flag-tagged p300 in nuclear extract of transfected cells **D)** Mammalian two-hybrid assay using Gal4MyoD and C/H3 p300 VP16 cotransfected along with Gal4-luciferase reporter in MEFs from wild type, AKT1 and AKT2 null mice **E)** ChIP analysis of Ebox-containing regions within the MCK enhancer was performed on chromatin of MEFs from wt, AKT 1 and 2 knock-out (KO) or MKK3/6 double KO mice, after adenoviral-mediated delivery of MyoDand culture in DM for 48 hours. The values shown in A, B, D and E represent the average of standard error of three independent experiments

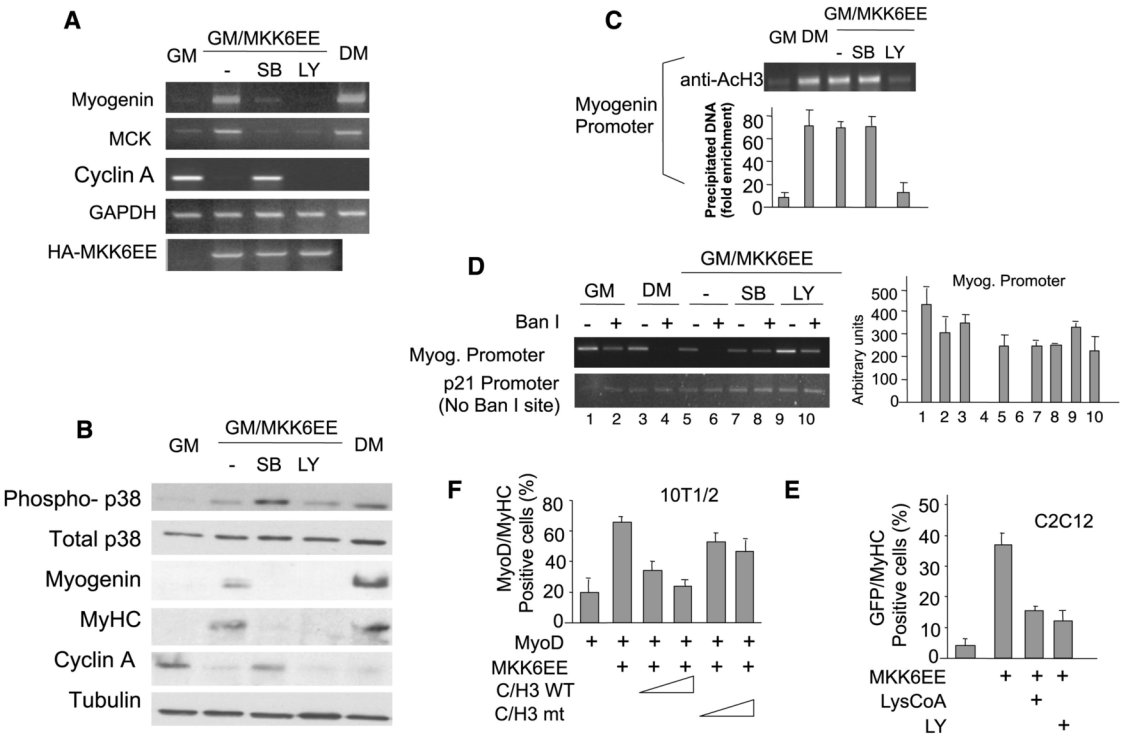

Fig. 6. Functional interdependence at the chromatin level between the IGF1 and the p38 pathways

The p38 pathway was stimulated in C2C12 myoblasts (GM) by ectopic expression of the constitutive active form of the p38 upstream kinase, HA-MKK6EE, via adenoviral infection **A)** Expression level of myogenin, MCK, cyclin A, GAPDH and MKK6EE-HA transcripts was evaluated by RT-PCR. **B)** Activation of endogenous p38 (total and phosphorylated form)**,** expression of myogenin, MyHC, cyclin A and tubulin were evaluated by western blot **C)** ChIP analysis of Ebox-containing regions within the myogenin promoter was performed using anti-acetyl H3 antibodies **D)** Endonuclease assay of myogenin promoter and p21 promoter (control). The intensity of the amplified fragment was visualized (botton panel, left) and quantified by densitometric analysis (bottom panel, right). **E)** Nuclei of C2C12 myoblasts (GM) were microinjected with a mixture of cDNA coding GFP (as an indicator of productive injection) and MKK6EE or empty vector, in the absence or presence of the p300 inhibitor LysCoA (0.5 mM) and the expression of the endogenous differentiation marker, MyHC, was analyzed by immunofluorescence after 48 hours. The percentage (%) of GFP/myogenin double positive cells, among the GFP positive cells, is reported as an index of differentiation. **F)** 10T1/2 fibroblasts were converted by transfection of MyoD, and the effect of co-expression of MKK6EE and increasing amounts of C/H3 p300 (either wt or the phosphorylation resistant double mutant) was analyzed after 48 hours of incubation in DM. The expression of MyHC was analyzed by immunofluorescence. The % of MyoD/myogenin double positive cells, among the MyoD positive cells, is reported as an index of differentiation. The values shown in C, D, F and E represent the average of standard error of three independent experiments

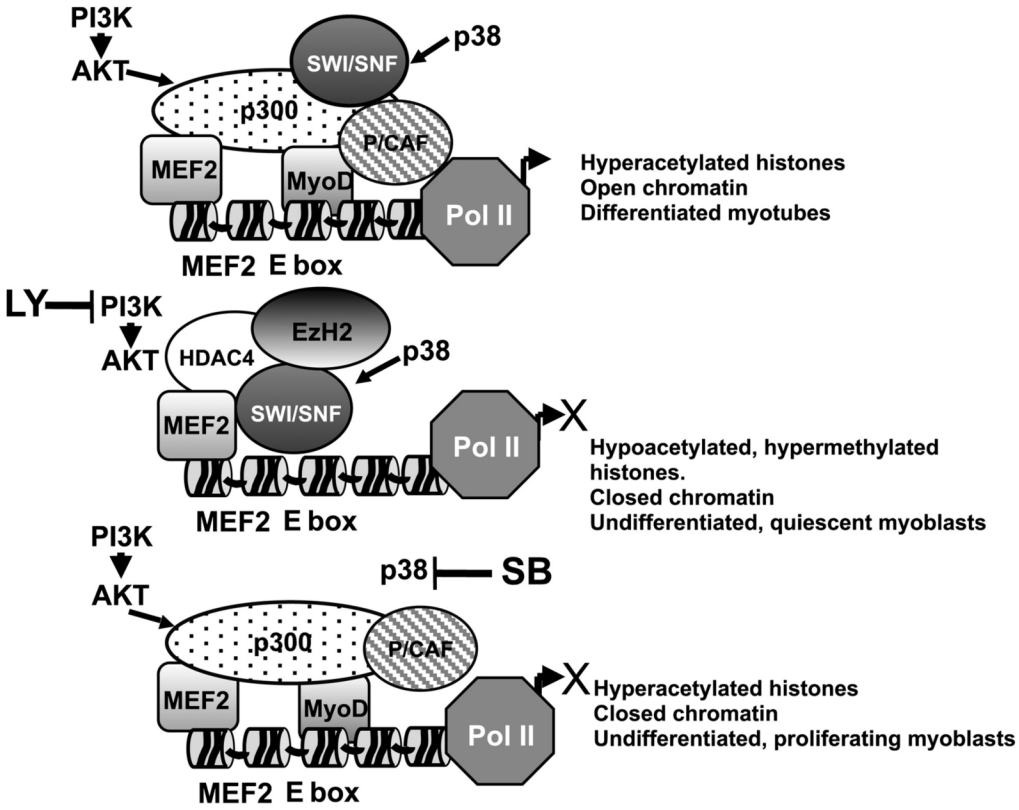

Fig. 7.

Illustration of the composition of muscle transcriptosome on the chromatin of muscle genes that reflects different chromatin status and distinct cellular phenotypes generated in response to Pi3K or p38α/β inhibition, as compared to untreated cells.